Iron Cluster and Microstructure Formation in Metal-Centered Star Block Copolymers: Amphiphilic Iron Tris(bipyridine)-Centered Polyoxazolines

Cheolmin Park,[†,§] John E. McAlvin,[‡] Cassandra L. Fraser,[‡] and Edwin L. Thomas*[,†]

Department of Materials Science and Engineering, Massachusetts Institute of Technology, Cambridge, Massachusetts 02139, and Department of Chemistry, University of Virginia, McCormick Road, P.O. Box 400319, Charlottesville, Virginia 22904-4319

Received August 14, 2001. Revised Manuscript Received November 16, 2001

The microstructure of a metal-centered six-arm star block copolymer, amphiphilic iron tris(bipyridine)-centered poly(2-ethyl-2-oxazoline)-*b*-poly(2-undecyl-2-oxazoline), $[Fe\{bpy-(PEOX-PUOX)_2\}_3]^{2+}$, was investigated with small-angle X-ray scattering (SAXS), wide-angle X-ray scattering (WAXS), transmission electron microscopy (TEM), and atomic force microscopy (AFM). Cylindrical PEOX microdomains were observed in a matrix of PUOX. A similar cylindrical morphology was noted for $bpy(PEOX-PUOX)_2$, the metal-free macroligand subunit of which the Fe star is comprised. Thin films simple-cast from chloroform solution onto carbon substrates annealed at 160 °C for ≈2 days revealed in both TEM and AFM the formation of nanoscale iron clusters (≈20−40-nm diameter) distributed randomly across the surface of the film. No clusters were evident in "as-cast" films subjected to TEM analysis without the annealing step, suggesting the importance of thermal treatment for nanocrystal formation. For bulk films, larger micrometer-scale (1−2 μm) iron aggregates formed and segregated to the surface of the film after thermal treatment for ≈1 week. A liquid crystal-like mesophase due to undecyl alkyl side chain ordering was evidenced by SAXS and WAXS in the bulk sample.

Introduction

Both natural and synthetic materials can be generated by the self-assembly of polymeric and inorganic components into hierarchical microstructures. In shell[1] and bone formation,[2] proteins function as directing and templating molecules for biomineralization, often lending important structural and mechanical properties to the composite material. In metal storage systems such as ferritin,[3] proteins form a protective assembly surrounding metal aggregates.[3] Synthetic application of the hierarchical design strategy is evident in the ever-expanding array of nanostructure fabrication schemes.[4−7] When inorganic sol−gel processes have been coupled with polymers, bicontinuous nanoscale porous channels have been constructed.[4] Magnetic fibers have been generated by coating spider silk with Fe_3O_4 magnetite.[5] The reactive features of metal complexes have been incorporated into nanometer-scale clusters for catalysis,[6] whereas the unique optical properties of metals have been exploited in DNA detection schemes with gold nanoparticles, thus serving as a useful new tool for biotechnology.[7]

Block polymers are of great interest as a design motif because they readily self-assemble to create one-, two-, and three-dimensional (1D, 2D, and 3D, respectively) periodic nanometer-scale microdomain structures.[8] These hybrid systems consist of two or more chemically distinct macromolecular segments that are joined, most commonly by covalent bonds, to form a single chain. Owing to their mutual repulsion, dissimilar blocks tend to segregate into different domains, the spatial extent of which is limited by the constraints imposed by the chemical connectivity of the blocks, their compositions, and respective molecular weights. Minimization of interfacial area and maximization of chain conformational entropy give rise to periodically arrayed microdomains, whose dimensions scale with the two-thirds of power of the molecular weight. In contrast to linear block copolymers, only a few studies of the solid-state morphology of star block copolymers have been conducted.[9−11] For example, Alward et al. discovered a

* To whom correspondence should be addressed. Tel.: 617-253-6901. Fax: 617-258-6135. E-mail: elt@mit.edu.
† Massachusetts Institute of Technology.
‡ University of Virginia.
§ Present address: Department of Chemistry and Chemical Biology, Harvard University, 12 Oxford Street, Cambridge, MA 02138.

(1) Zaremba, C. M.; Belcher, A. M.; Fritz, M.; Li, Y. L.; Mann, S. *Chem. Mater.* **1996**, *8*, 679.
(2) Dabbs, D. M.; Aksay, I. A. *Annu. Rev. Phys. Chem.* **2000**, *51*, 601.
(3) Gider, S.; Awschalom, D. D.; Douglas, T.; Wong, K.; Mann, S.; Cain, G. *J. Appl. Phys.* **1996**, *79*, 5324.
(4) Finnefrock, A. C.; Ulrich, R.; Du Chesne, A.; Honeker, C. C.; Schumacher, K.; Unger, K. K.; Gruner, S. M.; Wiesner, U. *Angew. Chem., Int. Ed.* **2001**, *40*, 1207.
(5) Mayes, E. L.; Vollrath, F.; Mann, S. *Adv. Mater.* **1998**, *10*, 801.
(6) El-Sayed, M. A. *Acc. Chem. Res.* **2001**, *34*, 257−264.
(7) Taton, T. A.; Lu, G.; Mirkin, C. A. *J. Am. Chem. Soc.* **2001**, *123*, 5164.
(8) Muthukumar, M.; Ober, C. K.; Thomas, E. L. *Science* **1997**, *277*, 1225.
(9) Alward, D. B.; Kinning, D. J.; Thomas, E. L.; Fetters, L. J. *Macromolecules* **1986**, *19*, 215.

10.1021/cm010731d CCC: $22.00
Published on Web 01/11/2002

transition in equilibrium domain morphology of poly(styrene−isoprene) star block copolymers having 30 wt % polystyrene outer blocks from the normally observed cylindrical morphology to an ordered bicontinuous (OB) structure upon increasing the number of arms.[9] The transition occurred sharply from a cylindrical morphology in a five-arm block copolymer to an OB in a six-arm block copolymer.[10] Tselikas et al. demonstrated that the star architecture could induce a morphological transition from lamellae to a tricontinuous cubic structure at overall symmetric composition.[11]

To achieve more elaborate hierarchical structures with block copolymers, additional types of interactions are required. Semicrystalline and liquid-crystalline block copolymers have been extensively investigated to this end. Crystallization or liquid crystallization of one of the blocks successfully confined to a discrete microdomain has provided multi-length-scale complex structures.[12,13] Hierarchical organization has also been observed for block copolymer/surfactant complexations. For example, hydrogen-bonding interactions between poly(vinyl pyridine) and hydroxyl group-terminated surfactants successfully created a smectic meso structure within a lamellar block copolymer.[14]

Micropatterned block copolymer structures have also been used to sequester small organic and inorganic particles, including metallic ones, into selected microdomains.[15−17] The selective dispersion of quantum dots in microdomains within functionalized polynorbornene block copolymers was achieved by controlling the affinity between the block and quantum dot surface.[15,16] In addition, block copolymer microdomains have been used as nanoscale reactors in which small-scale particles are templated and grown.[18−22] For example, nanometer-scale platinum and palladium catalysts were generated and stabilized by the polystyrene core of polystyrene-*b*-ethylene oxide block copolymer micelles.[20] And recently, electroless deposition of metals into selective microdomains has been performed to provide continuous material loading.[21,22] Most previous work of this nature utilizes chemical or physical interactions between metal particles or precursors and particular blocks. Less common are systems in which the metal forms an integral structural feature of the polymer backbone or the metallic components originate from the polymer itself. A notable example of the latter case, are polymers formed from anionic ring-opening polymerization of ferrocenyldimethylsilane monomers.[23,24]

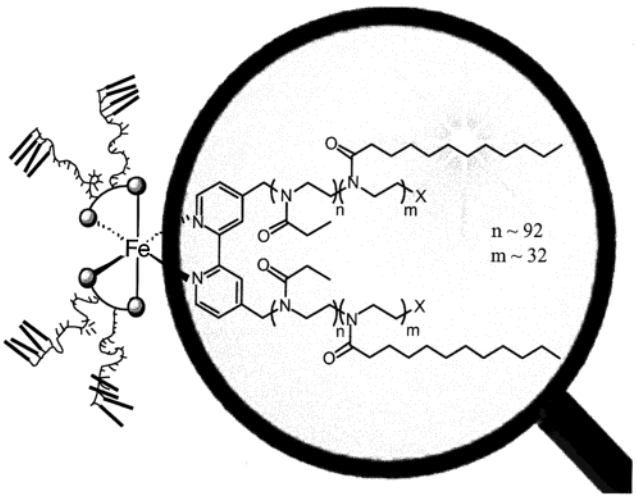

Figure 1. Schematic representation of iron-centered star block copolymers, $[Fe\{bpy(PEOX-PUOX)_2\}_3]^{2+}$ (**1**) with the molecular structure of one bpy-centered triblock copolymer macroligand $bpy(PEOX-PUOX)_2$ (**3**), highlighted. The approximate degrees of polymerization for each block comprising the star polymer arms are indicated.

Recently, we synthesized novel metal-centered block copolymers by a metalloinitiation approach.[25−27] A variety of related materials are readily accessible from metal salts and preformed macroligands by a modular metal template approach.[25] Iron tris(bipyridine)-centered polyoxazoline star block copolymers were generated from halide-functionalized metalloinitiators by sequential addition of two different 2-R-2-oxazoline monomers, where R = ethyl, undecyl, phenyl, and so forth. To explore the ability of these inorganic−organic hybrid systems to form hierarchical assemblies and their potential to function as templates for mineralization, we selected the iron-centered polyoxazolines with ethyl and undecyl side chains for study (Figure 1). Not only are these polymers multifunctional and amphiphilic but also the undecyl side chains induce a thermodynamic phase transition. Herein, we report that "crystallization" of the 11-carbon alkyl side chains occurs in the matrix between discrete cylindrical domains. As the integral core of the star block copolymer architecture, the metal ion will be selectively positioned within one microdomain and not the other in ordered films, provided that the stars remain intact. But because Fe(II) is a labile ion, the linkages between the bipyridine-centered triblock copolymer chains and the metallic star polymer core may break, allowing metals to migrate and react to form clusters upon thermal treatment. The structures of the iron-centered polyoxazoline films were investigated by a variety of techniques: by microscopy (TEM, AFM) and by small-angle X-ray scattering (SAXS)

(10) Kinning, D. J.; Thomas, E. L.; Alward, D. B.; Fetters, L. J.; Handlin, D. L. *Macromolecules* **1986**, *19*, 1288.
(11) Tselikas, Y.; Hadjichristidis, N.; Lescanec, R. L.; Honeker, C. C.; Wohlgemuth, M.; Thomas, E. L. *Macromolecules* **1996**, *29*, 3390.
(12) Quiram, D. J.; Register, R. A.; Marchand, G. R.; Adamson, D. H. *Macromolecules* **1998**, *31*, 4891.
(13) Osuji, C.; Zhang, Y. M.; Mao, G. P.; Ober, C.; Thomas E. L. *Macromolecules* **1999**, *32*, 7703.
(14) Ruokolainen, J.; Torkkeli, M.; Serimaa, R.; Komanschek, E.; ten Brinke, G.; Ikkala, O. *Macromolecules* **1997**, *30*, 2002.
(15) Fogg, D. E.; Radzilowski, L. H.; Dabbousi, B. O.; Schrock, R. E.; Thomas, E. L.; Bowendi, M. G. *Macromolecules* **1997**, *30*, 8433.
(16) Fogg, D. E.; Radzilowski, L. H.; Blanski, R.; Schrock, R. E.; Thomas, E. L.; Bowendi, M. G. *Macromolecules* **1997**, *30*, 417.
(17) Fink, Y.; Urbas, A.; Bawendi, B. G.; Joannopoulos, J. D.; Thomas, E. L. *J. Lightwave Technol.* **1999**, *17*, 1963.
(18) Mayer, A. B. R.; Mark, J. E. *Colloid Polym. Sci.* **1997**, *275*, 333.
(19) Templin, M.; Frank, A.; Du Chesne, A.; Leist, H.; Zhang, Y.; Ulrich, R.; Schadler, V.; Wiesner, U. *Science* **1997**, *278*, 1795.
(20) Hashimoto, T.; Tsutsumi, K.; Funaki, Y. *Langmuir* **1997**, *13*, 6869.
(21) Zehner, R. W.; Sita, L. R. *Langmuir* **1999**, *15*, 6139.
(22) Boontongkong, Y.; Cohen, R. E.; Rubner, M. F. *Chem. Mater.* **2000**, *12*, 1628.
(23) Massey, J. A.; Power, K. N.; Winnik, M. A.; Manners, I. *Adv. Mater.* **1998**, *10*, 1559.
(24) Lammertink, R. G. H.; Hempenium, M. A.; van den Enk, J. E.; Chan, V. Z.-H.; Thomas, E. L.; Vancso, G. J. *Adv. Mater.* **2000**, *12*, 98.
(25) Fraser, C. L.; Smith, A. P. *J. Polym. Sci, Part A: Polym. Chem.* **2000**, *38*, 4704.
(26) McAlvin, J. E.; Fraser, C. L. *Macromolecules* **1999**, *32*, 1341.
(27) McAlvin, J. E.; Scott, S. B.; Fraser. C. L. *Macromolecules* **2000**, *33*, 6953.

and wide-angle X-ray scattering (WAXS) both for the as-cast samples and for annealed samples.

Experimental Methods

Iron-centered polyoxazoline block copolymers, $[Fe\{bpy(PEOX\text{-}PUOX)_2\}_3]^{2+}$ (**1**), $[Fe\{bpy(PUOX\text{-}PEOX)_2\}_3]^{2+}$ (**2**), their respective bpy-centered triblock copolymer macroligands, $bpy(PEOX\text{-}PUOX)_2$ (**3**) and $bpy(PUOX\text{-}PEOX)_2$ (**4**), and a homopolymer $[Fe(bpyPEOX_2)_3]^{2+}$ (**5**) were prepared and molecular weights were determined as previously described.[26] Schematics of chain architectures for Fe-centered star block copolymers **1** and **2** and molecular structures of block copolymer macroligands **3** and **4** are shown in parts a and b of Figure 1, respectively. Molecular weight data for the labile Fe-centered stars **1** and **2** were calculated from their constituent macroligands **3** and **4**. Data are as follows. (**1**): Calcd MW Fe PEOX−PUOX star block, 97 800 (first block Fe PEOX homopolymer star, 55 300). (**2**): Calcd MWs Fe PUOX−PEOX star block, 66 300 (first block Fe PUOX homopolymer star, 35 100). Macroligand MW data determined by MALLS are as follows. (**3**): $M_n = 32\,600$, $M_w = 34\,700$, PDI = 1.07 (first block PEOX macroligand: $M_n = 18\,400$, $M_w = 20\,800$, PDI = 1.13). (**4**): $M_n = 22\,100$, $M_w = 22\,800$, PDI = 1.03 (first block PUOX macroligand: $M_n = 11\,700$, $M_w = 14\,000$, PDI = 1.20). (**5**): Calcd MW Fe PEOX star polymer, 55 300 (PEOX macroligand MW data by MALLS: $M_n = 18\,400$, $M_w = 20\,800$, PDI = 1.13).

Thin films (≈30-nm thick) were cast on carbon-coated 200-mesh TEM copper grids from 0.1 wt % chloroform solution. In the same way, thin films were made on glass substrates for examination by AFM. Isotropic thick films (1-mm thickness) of the block copolymers were also made by simple casting from chloroform solutions containing 5 wt % polymer at room temperature for TEM and SAXS.

The cast films were dried in a vacuum oven at 40 °C for 1 day to remove the solvent. The isotropic 1-mm-thick films were then annealed for an additional 7 days under vacuum at 160 °C in an oxygen-free glovebox, significantly above both the glass transition temperatures of both polymers (≈60 °C) and above the typical T_m range (≈120−140 °C) for PUOX determined at a heating rate of 10 °C/min.[26] Thin films were also annealed for 2 days under vacuum at the same temperature in an oven. To minimize exposure of the block copolymer film to oxygen, the vacuum oven was loaded with the sample, evacuated by a mechanical pump at room temperature, and then its temperature slowly elevated.

The thick films were embedded in the epoxy solution (Eponide 12) and cured for 1 day at 60 °C. Thin sections of the annealed films were prepared for TEM using a Reichert-Jung FC4E Ultracut microtome. Some samples were subsequently stained for 1 h with RuO_4. As-cast and annealed thin films prepared on TEM grids were also stained for 1 h with RuO_4. Both stained and unstained samples were examined with a JEOL 200 CX microscope operated at 200 kV in bright-field mode.

The surface topologies of the thin films were examined with a Nanoscope III AFM in tapping mode. Height and phase contrast images were simultaneously collected. Energy-dispersive X-ray spectroscopy (EDX) was done without additional coating of the sample with a JEOL 330 field emission scanning electron microscope (SEM) operated at 5 kV.

Simultaneous WAXS and SAXS measurements were also carried out at the Advanced Polymers Beamline, X27C, National Synchrotron Light Source, Brookhaven National Laboratory. The wavelength used was $\lambda = 0.1307$ nm, and the beam size was about 0.4 mm in diameter at the sample position. A three 2° tapered tantalum pinhole collimation system was utilized with a sample-to-detector distance of 1560 and 108 mm for SAXS and WAXS patterns, respectively. Scattering angles, 2θ, down to 1.5 mrad corresponding to a Bragg spacing ($d = 2\pi/q$ where $q = 4\pi \sin\theta/\lambda$) of about 100 nm were achieved. A single-cell heating stage (maximum temperature: 350 °C) was used for high-temperature measurements. Fuji imaging plates were used to collect the scattering data with exposure times of 1 min/frame.

Results and Discussion

Bright-field TEM micrographs of the thin films (≈30 nm) of the $[Fe\{bpy(PEOX-PUOX)_2\}_3]^{2+}$ block copolymer annealed at 160 °C for various times are shown in Figure 2. Similar results were obtained for thin film samples annealed at 160 °C for times ranging from 2 to 7 days. A bright-field TEM micrograph of the stained sample, shown in Figure 2a,b, clearly displays both the microdomain structure and randomly distributed nanoscale clusters with sizes ranging from 20 to 40 nm. Staining for 1 h with RuO_4 provided good contrast. This may be attributable to different diffusivities of the staining agent in the amorphous PEOX and crystalline PUOX microdomains and/or to the chemical affinity of RuO_4 for the amide group in the block copolymer main chain.[28,29] Because there are more amide residues in the PEOX blocks than in the PUOX segments, we speculate that the dark circular areas correspond to the PEOX microdomains. These dark convex-shaped microdomains are ≈15 nm in diameter and spaced about 27 nm apart. The orientation of the PEOX microdomains changes with local film thickness.[30] In the thinnest area, shown in Figure 2b, most of the PEOX cylinders are vertically aligned relative to the carbon substrate, but in the thicker regions, vertical and parallel orientations are both observed. Nanoscale clusters generally appear randomly distributed; however, local preference to PEOX microdomains is observed as shown in Figure 2a. A bright-field TEM micrograph of the unstained, annealed sample, shown in Figure 2c, visualizes only the nanoscale clusters. Amplitude contrast makes iron clusters with higher electron density appear dark.

The thin film microstructure of the constitutive metal-free block copolymer, $bpy(PEOX-PUOX)_2$, was also examined by TEM. A similar poorly ordered microdomain microstructure was observed. However, no clusters are observed in the unstained sample (data not shown), indicating that these originate from the Fe at the center of the star block copolymer. In addition, an as-cast $[Fe\{bpy(PEOX-PUOX)_2\}_3]^{2+}$ thin film sample does not show any aggregates when examined in TEM, implying that annealing is another important factor for developing the iron-containing aggregates (Figure 2d).

The location of the small clusters was also examined by AFM in tapping mode. The height contrast AFM image of the thin film, shown in Figure 3a indicates that clusters are clearly evident on the film surface. The degree of protrusion of the clusters from the polymer surface ranges from ≈4 to 7 nm. In addition, the phase contrast AFM image (Figure 3b) simultaneously obtained shows that those small clusters on the surface have a higher elastic modulus than the surrounding block copolymer surface.

The detailed microstructure of the $[Fe\{bpy(PEOX-PUOX)_2\}_3]^{2+}$ block copolymer and the identity of the small nanoscale clusters were investigated with thick

(28) Berkowitz, L. M.; Rylander, P. N. *J. Am. Chem. Soc.* **1958**, *80*, 6682.

(29) Lee, D. G.; van den Engh, M. In *Oxidation in Organic Chemistry Part B*; Trahanovsky, W. S., Ed.; Academic Press: New York, 1973; Chapter IV, p 225.

(30) Konrad, M.; Knoll, A.; Krausch, G.; Maglerle, R. *Macromolecules* **2000**, *33*, 5518.

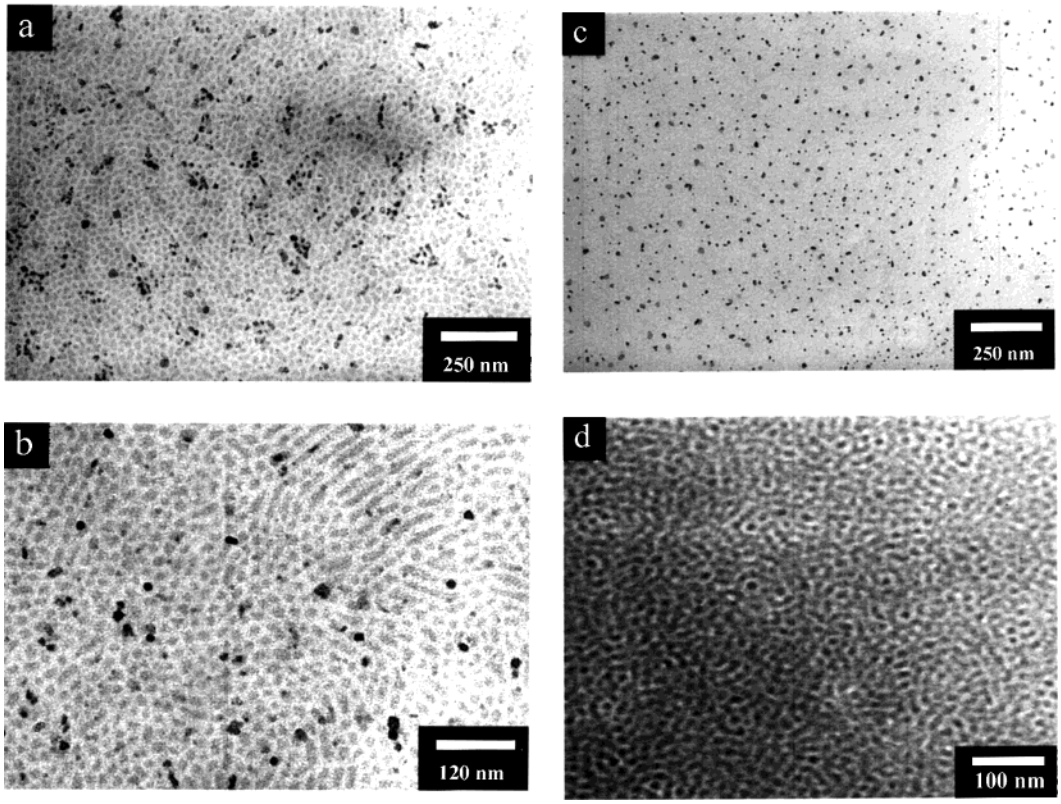

Figure 2. Bright-field TEM plan view images of the thin films of the $[Fe\{bpy\{PEOX-PUOX)_2\}_3]^{2+}$ block copolymer (**1**). (a) Stained, annealed sample displays both small clusters with the size of ≈20−40 nm and a cylindrical PEOX microdomain structure. Thinner regions of the stained, annealed sample with the thickness of ≈20 nm reveal a monolayer of PEOX cylinders vertically oriented on the supporting carbon film. Small clusters are also evident. (b) A mixture of cylinders aligned both perpendicular and parallel with respect to the substrate (upper right region of micrograph) is observed in some areas of the stained sample. (c) Unstained, annealed sample only shows a small cluster structure. (d) As-cast film (no annealing) with RuO_4 staining shows a disordered cylindrical PEOX microdomain structure without small clusters.

bulk samples. The SAXS intensity profile of the $[Fe\{bpy(PEOX-PUOX)_2\}_3]^{2+}$ block copolymer, shown in Figure 4a, displays a stong first-order peak at $q \approx 0.23$ nm^{-1}, two weak higher order reflections observed around $q \approx 0.4$ nm^{-1} and $q \approx 0.46$ $nm^{-1,}$ and a strong broad reflection at $q \approx 2.12$ nm^{-1}, indicating the presence of a microphase-separated structure of the block copolymer and another smaller scale mesophase structure. The average repeat distance corresponding to the first-order reflection is ≈27 nm, consistent with intercylinder spacing determined in the thin film. The set of Bragg peaks have approximate q_n/q_1 values of 1.0, $\sqrt{3}$, and $\sqrt{4}$, which corresponds to a hexagonal packing. The reflection corresponding to a spacing of 2.9 nm likely results from the "crystallization" of an undecyl side chain in PUOX blocks.[26] In a previous study, we observed an endothermic transition around 120 °C due to the presence of PUOX blocks and concluded that PUOX blocks undergo "crystallization", based on differential scanning calorimetry (DSC) data.[26] The SAXS profile of the block copolymer at 150 °C in Figure 4b shows the absence of the 2.9-nm peak without any shifts of the first reflection position, confirming that the reflection is related to a mesophase structure of the undecyl side groups in PUOX blocks. The constitutive metal-free block copolymer, $bpy(PEOX-PUOX)_2$ prepared under the same annealing conditions, shows a similar SAXS pattern, indicating that Fe ions or Fe clusters formed under these thermal conditions were not observed in SAXS. (See TEM data below.)

The SAXS profile at room temperature (Figure 4a) is similar to those obtained with side-chain liquid-crystalline block copolymers in which the liquid-crystalline domains are confined within the microphase-separated structures.[13] In the previous study, the smectic phase of side-chain liquid-crystal mesogens provided a reflection in the high q regime, corresponding to the molecular lengths.[13] The calculated fully extended length of the undecyl side chains is ≈1.5 nm, suggesting a bilayer structure. The WAXS profile taken simultaneously with SAXS did not reveal any crystalline reflections, indicating that these undecyl side chains pack into a smectic liquid-crystalline arrangement.

Interestingly, an analoguous Fe star block polymer of similar molecular weight and composition but with block positions reversed, $[Fe\{bpy(PUOX-PEOX)_2\}_3]^{2+}$ (**2**), showed no small-angle reflections, indicating a lack of ordered microdomain structure. However, SAXS evidence for the liquid-crystalline mesophase remained (data not shown).

A bright-field TEM micrograph of the microtomed, annealed bulk film $[Fe\{bpy(PEOX-PUOX)_2\}_3]^{2+}$ block copolymer (**1**) is shown in Figure 5. Similar dark convex-shaped PEOX microdomains, consistent with the 27-nm peak formed in SAXS (Figure 4a), are observed. The appearance of a cylindrical microstructure of the PEOX blocks despite ≈50% volume fraction of this component may be due to conformational asymmetry between the two blocks.[31] Although the lack of literature precedent

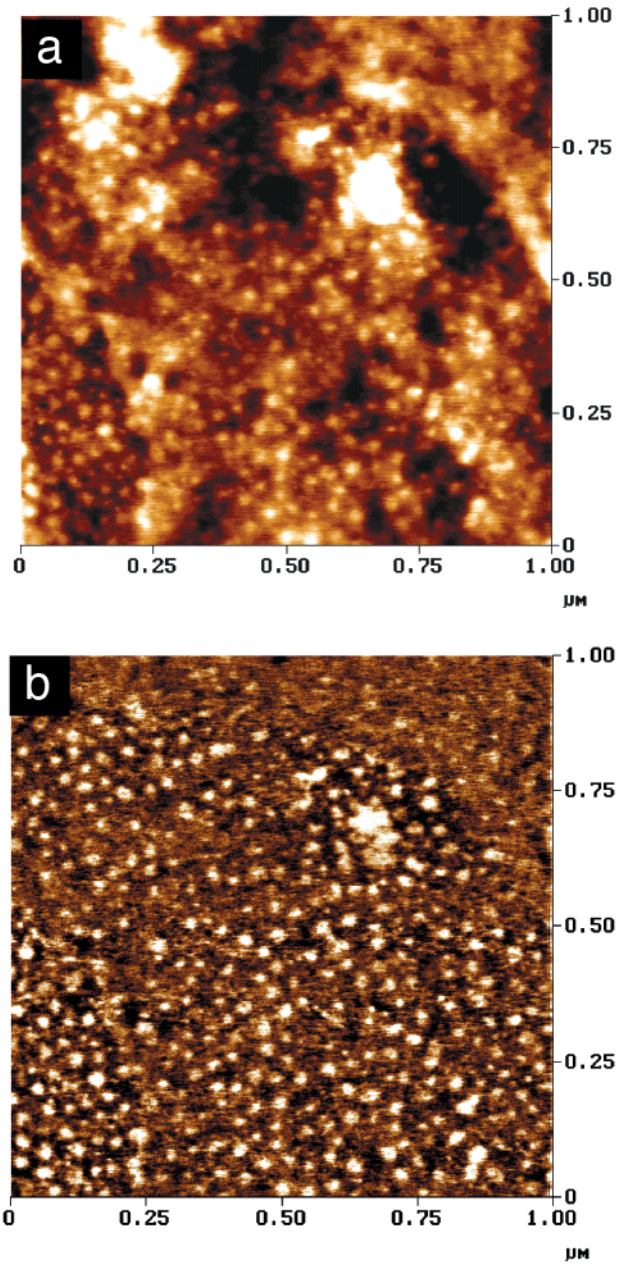

Figure 3. Tapping mode AFM images of the unstained thin film on a glass substrate. (a) Height contrast image. Small nanoscale clusters are clearly seen on the block copolymer film. (b) Phase contrast image. Small clusters look white in the phase mode, indicative of a higher elastic modulus.

for our block copolymer restricts further explanation in the current system, many examples with different block copolymers are seen in the literature.[32,33] For example, in our previous study, 13 vol % of polystyrene blocks form cylindrical microdomains in polystyrene-*block*-(polyethylene-*alt*-propylene)-*block*-polyethylene terpolymer even though, in theory, spherical microdomains are expected.[33]

To locate the iron ions that were originally present at the center of the star block copolymers, the unstained,

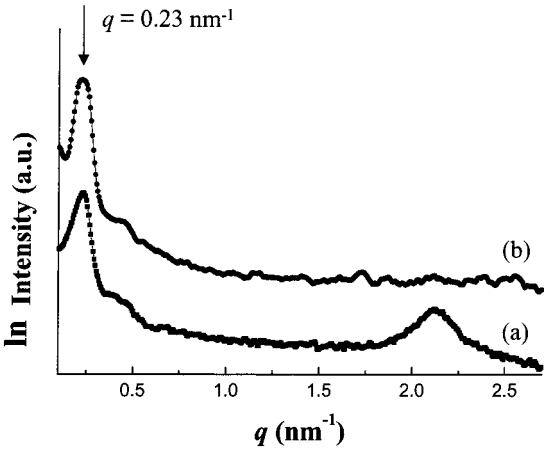

Figure 4. Small-angle X-ray diffraction profiles of a bulk sample of the $[Fe\{bpy(PEOX-PUOX)_2\}_3]^{2+}$ block copolymer (**1**) recorded at room temperature (a) and at 150 °C (b). Strong low-angle reflection and weak higher order peaks are shown in both profiles, indicating the presence of a microphase-separated structure. Disappearance of high q range reflection at 150 °C implies that the reflection is related to a thermal transition of the undecyl side chains in the PUOX blocks (see text).

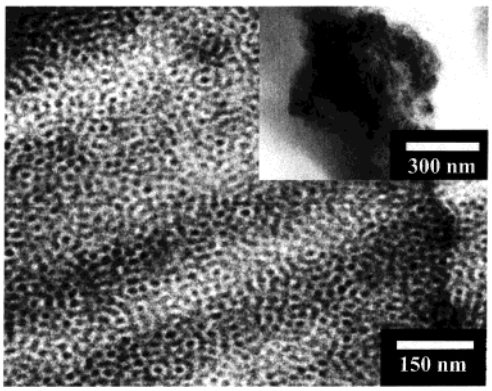

Figure 5. Bright-field TEM images of the annealed, microtomed sections of the RuO_4 stained $[Fe\{bpy(PEOX-PUOX)_2\}_3]^{2+}$ block copolymer (**1**). The inset shows a micrometer-size large iron-rich cluster in the unstained sample.

microtomed, thin film of the annealed $[Fe\{bpy(PEOX-PUOX)_2\}_3]^{2+}$ bulk sample was examined by TEM. The unstained film does not exhibit any fine-scale microdomain structure; however, large aggregates having an average diameter of $\approx 1\ \mu$m are found in various regions of the film as shown in the inset of Figure 5. Selected area diffraction on the cluster in TEM shows many sharp reflections that are typically observed for iron and/or iron-oxide clusters.

The clusters in both thin and bulk films likely arise from kinetically unstable bonding of the metal to the macroligand. Thus, when the block copolymer is annealed, the iron ions become mobile, aggregate, and oxidize, ultimately forming clusters of varying sizes. Because the affinity of Fe (in low oxidation states) for oxygen is very high, we can speculate that heating the sample when exposed to air allows oxidation to occur, leading to iron oxides such as Fe_2O_3 and FeO. Similar approaches have been taken with iron-based silaferrocene homopolymers to form materials containing Fe and Fe_xO_y nanoclusters upon thermal treatment.[34,35] Samples do not exhibit air sensitivity as solids or when dissolved

(31) Helfand, E. In *Developments in Block Copolymers*; Goodman, I., Ed.; Applied Science: New York, 1982, Vol 1.
(32) Lammertink, R. G. H.; Hempenius, M. A.; Thomas, E. L.; Vancso, G. J. *J. Polym. Sci.: Part B: Polym. Phys.* **1999**, *37*, 1009.
(33) Park, C.; Simmons, S.; Fetters, L. J.; Hsiao, B.; Yeh, F.; Thomas, E. L. *Polymer* **2000**, *41*, 2971.

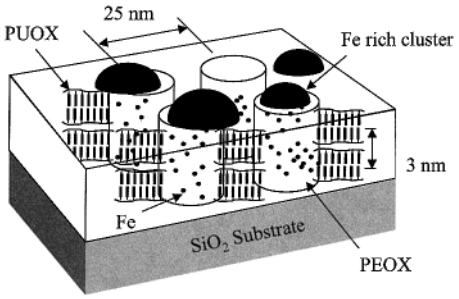

Figure 6. Schematic diagram of the microstructure of $[Fe\{bpy(PEOX-PUOX)_2\}_3]^{2+}$ (**1**) and the cluster formation on a thin block copolymer film showing a cylindrical microdomain structure for the PEOX block and a liquid crystal-like ordering of PUOX block. Mobile iron ions can react, diffuse out of the film, and aggregate with each other, resulting in small iron-rich clusters on the film surface.

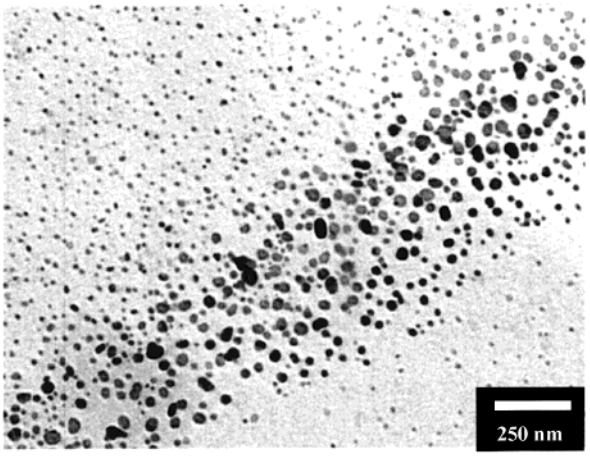

Figure 7. Bright-field TEM image of the thin films of the annealed homopolymer $[Fe(bpyPEOX_2)_3]^{2+}$ (5). Amplitude mass contrast in the unstained sample makes small iron-rich clusters appear black. The clusters with the diameter ranging from 20 to 80 nm are less evenly distributed than on the block copolymer thin film.

in inert solvents even over extended periods of time. Preliminary EDX spectroscopy data of these aggregates show that they are composed mostly of iron, appearing at ≈0.75 keV. Additionally, the EDX detected some X-ray of carbon near 1.7 keV from the block copolymer film. However, because of the limited resolution of EDX, detailed compositions of the aggregates were not obtained. Another important factor is the sensitivity of these samples to acid, even residual amounts of HCl in the solvent.[36] Protonation of the ligands destabilizes the complexes and makes the Fe ions more susceptible to reaction and, thus, migration in the film. In thin films, Fe may selectively migrate through vertically oriented PEOX domains for reaction with O_2 at the surface. The more polar PEOX regions may provide a more optimal environment for mobile Fe species and the clusters that form, thus accounting for their relatively uniform size and at least initial preference for PEOX microdomains. The thin film microstructure of the $[Fe\{bpy(PEOX-PUOX)_2\}_3]^{2+}$ block copolymer and cluster formation at one surface is schematically shown in Figure 6.

Additional experiments are underway to characterize the chemical composition and molecular structure of the iron-containing clusters as well as to investigate the kinetics of cluster growth. TEM images of thin films of the homopolymer $[Fe(bpyPEOX_2)_3]^{2+}$, as shown in Figure 7, also evidence iron clusters, but they are less evenly distributed and less uniform in size distribution ranging from 20 to 80 nm. For thin films of $[Fe\{bpy(PUOX-PEOX)_2\}_3]^{2+}$, a simple swapping of the outer and inner blocks, more chaotic microstructures were observed by AFM. These observations suggest that polymer composition in the vicinity of the metal centers and film morphology may be important and that the block copolymer may be playing a templating role in the mineralization. A more detailed study is required to determine this unequivocally.

Conclusion

The microstructure of a novel iron-containing $[Fe\{bpy(PEOX-PUOX)_2\}_3]^{2+}$ block copolymer was revealed using SAXS and TEM analysis. Despite the approximately symmetric volume fraction, the Fe star block copolymer forms convex microdomains of the PEOX blocks. During the annealing of thin films, the PEOX microdomains are better organized, forming short cylinders with a vertical orientation. Furthermore, iron ions originally located on the star center become mobile, react, and aggregate with each other to create uniform nanoscale (20−40 nm) iron clusters at the block copolymer microdomain−air interface. For bulk films, in contrast, micrometer-scale large iron-rich clusters formed upon annealing. In the thin films, the clusters appear to prefer the more polar PEOX domains. The placement of metal clusters on specific microdomain surfaces may be possible with different chemical compositions and morphologies of the block copolymer "nanoreactor" templates. These findings open up new possibilities for developing single-step fabrication of nanoscale patterned inorganic particles on polymer films, an important goal for many practical applications.

Acknowledgment. This research is supported by the National Science Foundation DMR98-07591 (MIT) and CHE-9733466 (UVA), the American Chemical Society Petroleum Research Fund, and the Jeffress Foundation. We gratefully acknowledge Mr. C. Osuji, Dr. F. Yeh, and Prof. B. Hsiao for their help at beamline X27C at Brookhaven National Laboratory. We would like to thank the MIT Center for Materials Science and Engineering for the use of its TEM facility. Mr. Adam P. Smith is thanked for his assistance with graphics.

CM010731D

(34) MacLachlan, M. J.; Ginzburg, M.; Coombs, N.; Coyle, T. W.; Raju, N. P.; Greedan, J. E.; Ozin, G. A.; Manners, I. *Science* **2000**, *287*, 1460.

(35) Sun, Q.; Lam, J. W. Y.; Xu, K.; Xu, H.; Cha, J. A. K.; Wong, P. C. L.; Wen, G.; Zhang, X.; Jing, X.; Wang, F.; Tang, B. Z. *Chem. Mater.* **2000**, *12*, 2617.

(36) Corbin, P. S.; Webb, M. P.; McAlvin, J. E.; Fraser, C. L. *Biomacromolecules* **2001**, *2*, 223.